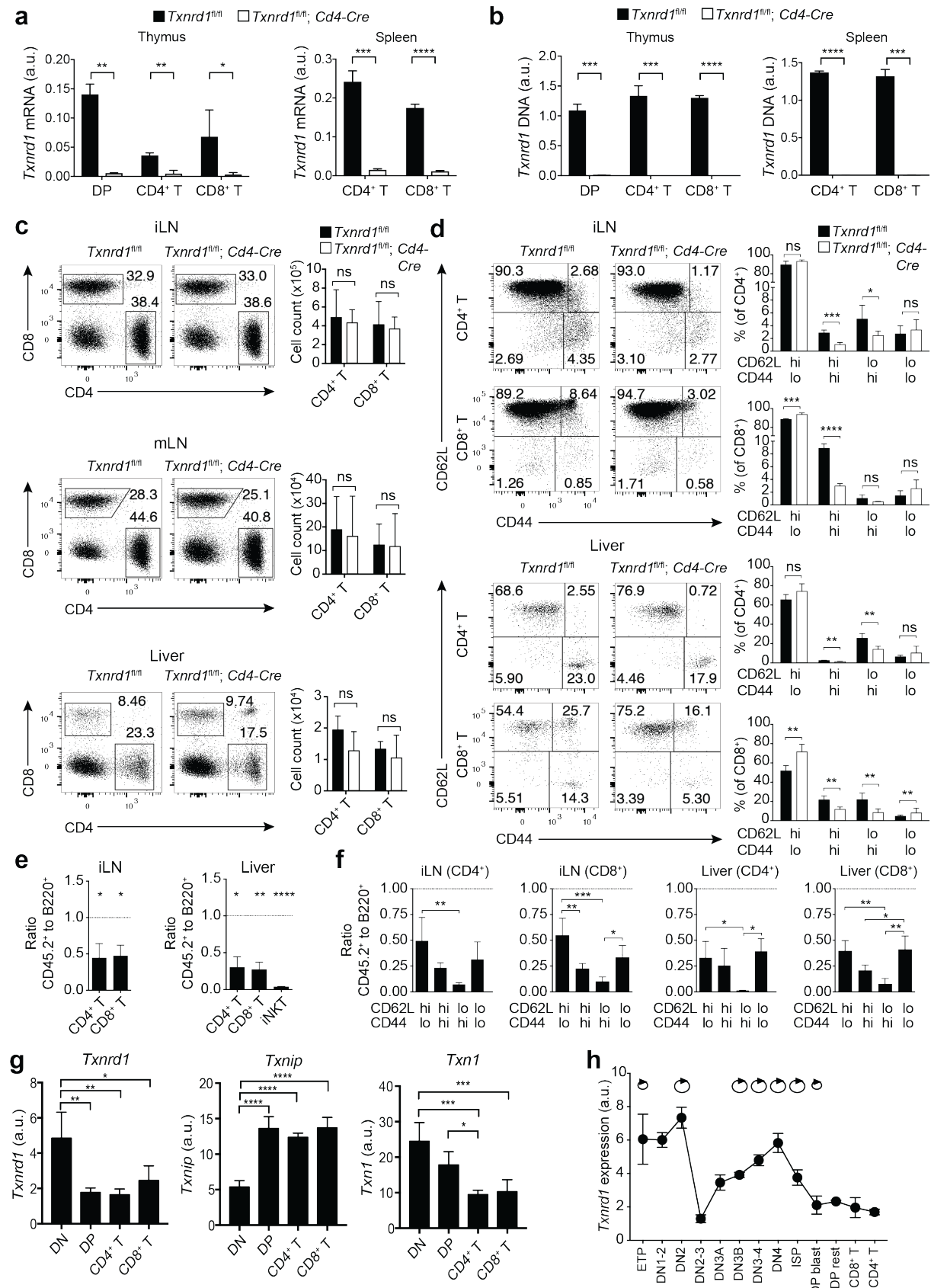


Supplementary Information

**The thioredoxin-1 system is essential for fueling DNA synthesis during T
cell metabolic reprogramming and proliferation**

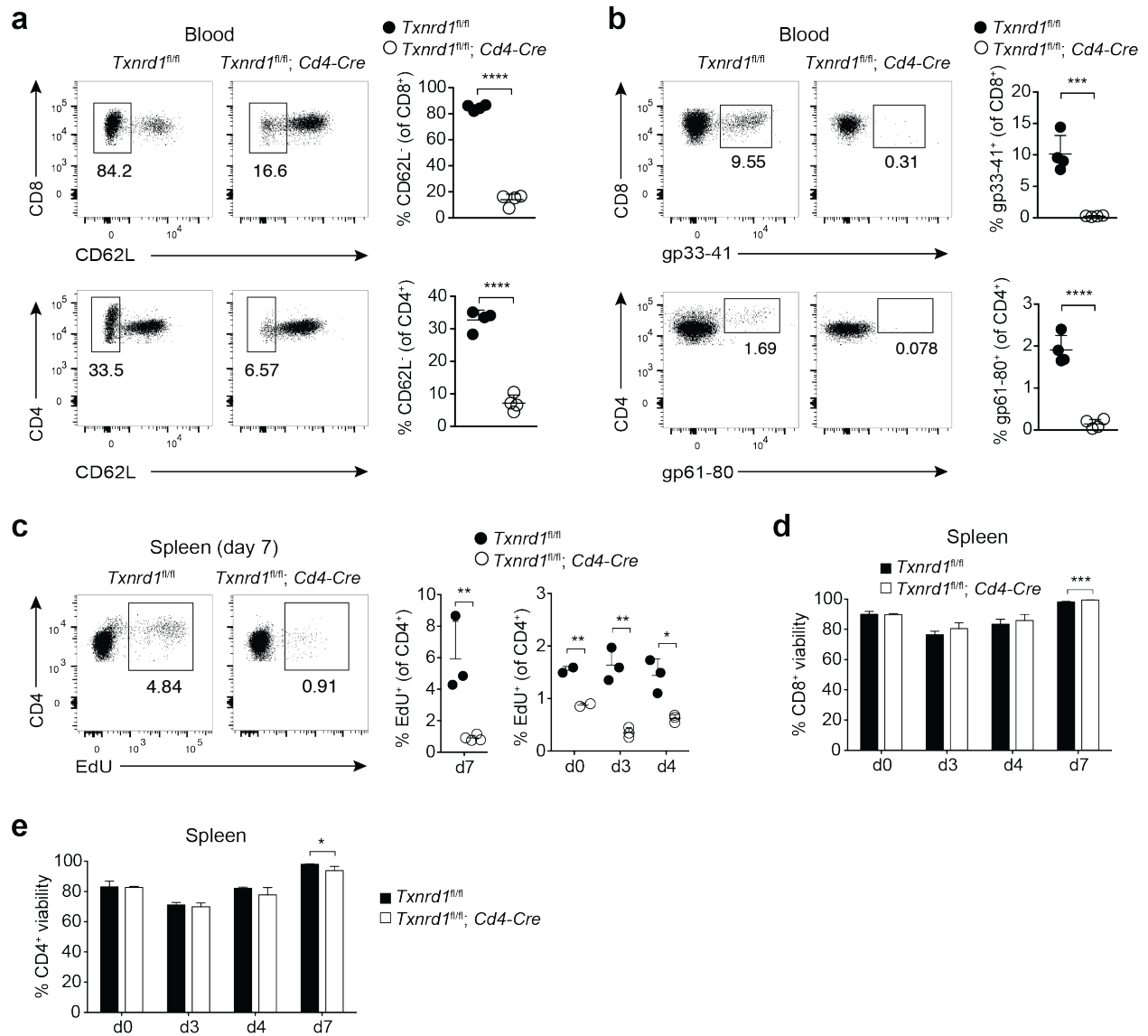
Muri et al.

Supplementary Figures

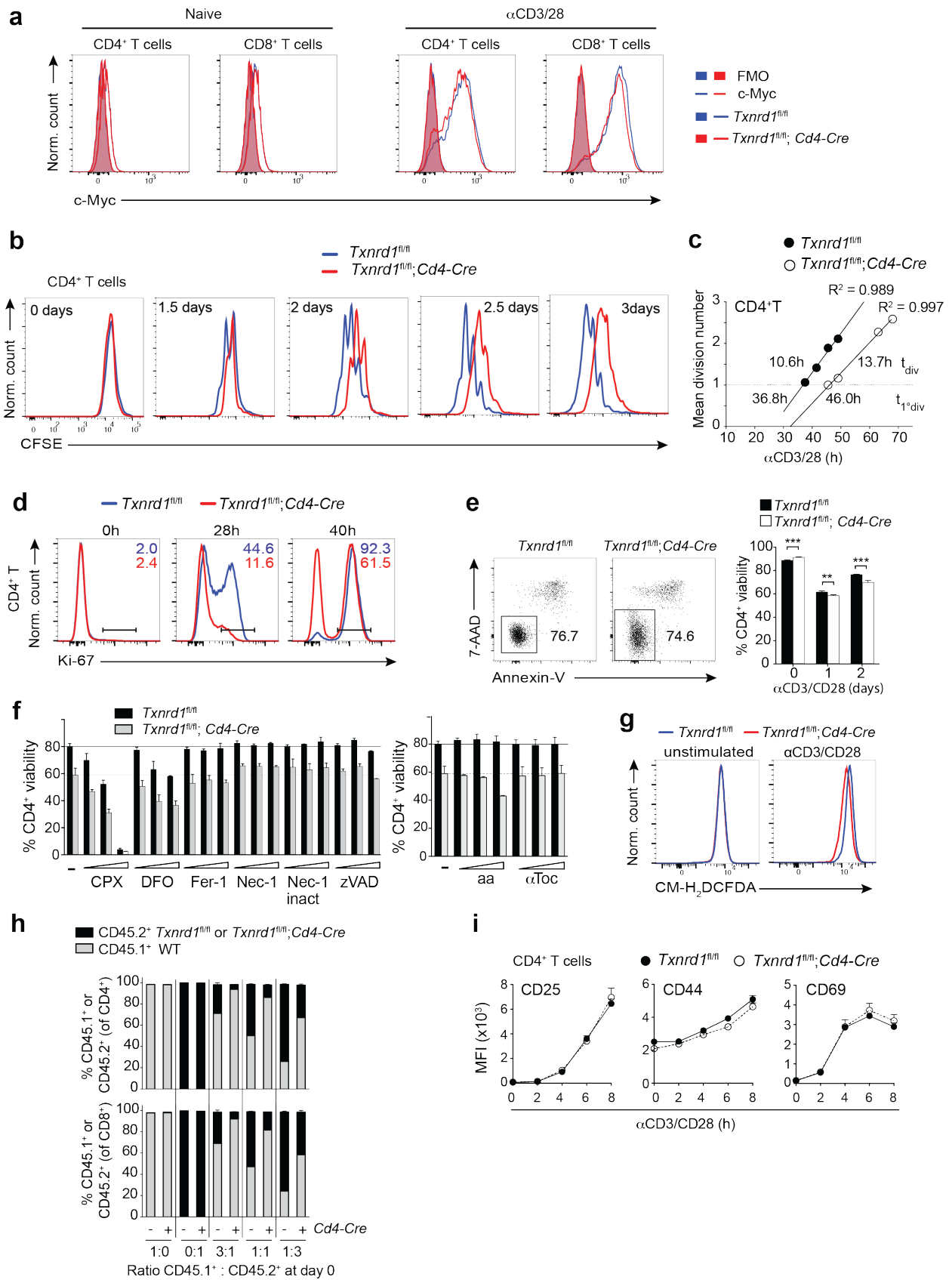


Supplementary Figure 1. *Txnrd1* is required for the generation of activated/memory T cells. (a, b) Analysis of *Txnrd1* mRNA (a) and genomic *Txnrd1* DNA (b) in DP and SP thymocytes (left), and splenic T cells (right) determined by RT-PCR (n=4). (c, d) Numbers and percentages of the indicated T cell populations were analyzed in naïve *Txnrd1^{fl/fl};Cd4-Cre* and *Txnrd1^{fl/fl}* littermate control mice. Representative FACS plots (left) and quantification (right) are shown (n=4-5). (c) CD4⁺ TCRβ⁺ (CD4⁺ T) and CD8⁺ TCRβ⁺ (CD8⁺ T) T cells in inguinal lymph nodes (iLN; top), mesenteric LNs (mLN; middle) and livers (bottom). (d) Expression of CD62L and CD44 in iLN (top) and liver (bottom) T cells. (e, f) Lethally irradiated WT mice were reconstituted with a 1:1 mixture of WT and *Txnrd1^{fl/fl};Cd4-Cre* bone marrow expressing the congenic markers CD45.1 and CD45.2, respectively. After reconstitution, the indicated T cell populations in iLN and liver from *Txnrd1^{fl/fl};Cd4-Cre* donor mice were normalized to non-Cre expressing CD45.2⁺CD19⁺ B cells. A value below 1 indicates a reduced contribution of *Txnrd1*-deleted T cells to the indicated population compared to WT cells (n=4). (g) Expression levels of *Txnrd1*, *Txnip* and *Txn1* determined by RT-PCR for sorted DN (CD4⁻CD8⁻TCRγδ⁻), DP (CD4⁺CD8⁺), CD4⁺ (CD4⁺CD8⁻TCRβ⁺) and CD8⁺ (CD8⁺CD4⁻TCRβ⁺) populations from WT mice (n=4). (h) Expression levels of *Txnrd1* determined by RT-PCR for the indicated FACS-sorted thymocyte populations from WT mice. Circular arrows indicate proliferating populations (n=4). Bar graphs show mean + standard deviation. Data are representative of two (a, b, e-h) and three (c, d) independent experiments. Student's *t* test (two-tailed, unpaired) was used to compare *Txnrd1^{fl/fl}* and *Txnrd1^{fl/fl};Cd4-Cre* groups (a-d): *, *P* ≤ 0.05; **, *P* ≤ 0.01; ***, *P* ≤ 0.001; ****, *P* ≤ 0.0001; ns, not significant. One-sample *t* test with a hypothetical value of 1 was used in (e): *, *P* ≤ 0.0332; **, *P* ≤ 0.0021; ****, *P* ≤ 0.0001. One-way ANOVA adjusted by Tukey's multiple comparison test was used in (f, g): *, *P* ≤ 0.05; **, *P* ≤ 0.01; ***, *P* ≤ 0.001.

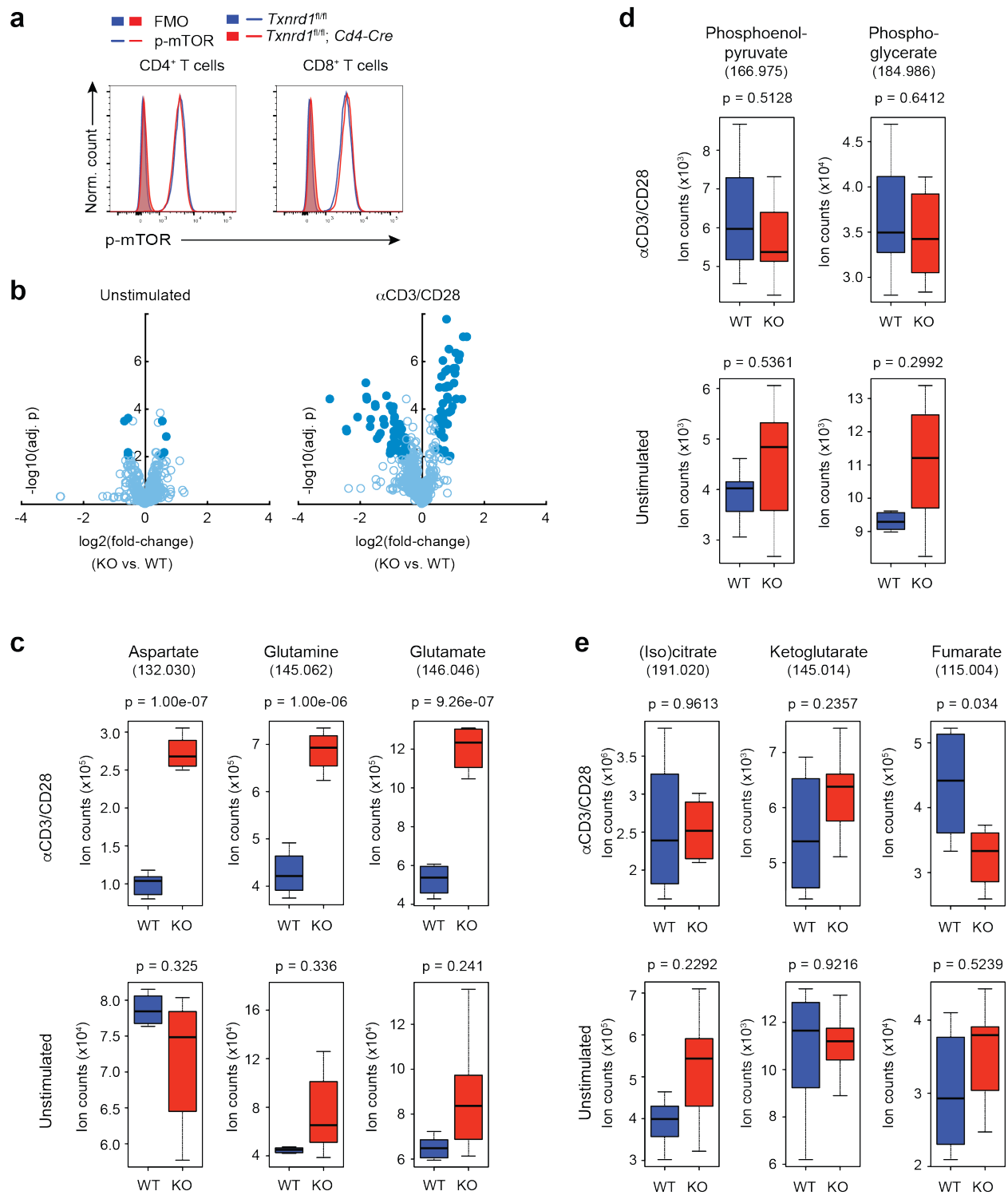
Supplementary Figure 2. *Txnrd1* is critically required for thymic T cell development. (a, b) Analysis of *Txnrd1* mRNA (a) and genomic *Txnrd1* DNA (b) in splenic T cells determined by RT-PCR (n=4). (c) Total numbers of the indicated thymic cell populations from WT, *Cre-ERT2*, *Txnrd1^{fl/fl}* and *Txnrd1^{fl/fl};Cre-ERT2* mice (n=4-5). (d, e) Lethally irradiated WT mice (CD45.1⁺) were reconstituted with a mixture (1:1) of WT (CD45.1⁺CD45.2⁺) and TAM-treated *Txnrd1^{fl/fl};Cre-ERT2* (CD45.2⁺) bone marrow (or *Txnrd1^{fl/fl}* as control). After reconstitution, the percentage of donor CD45.2⁺ cells among the indicated cell populations was determined by flow cytometry (n=4-5). Shown are the percentages of the indicated thymic T cell populations (d) and of CD4⁺ and CD8⁺ T cells in spleen, inguinal LN and liver (e). Bar graphs show mean + standard deviation. Data are representative of two independent experiments. Student's *t* test (two-tailed, unpaired) was used to compare *Txnrd1^{fl/fl}* and *Txnrd1^{fl/fl};Cre-ERT2* groups (a, b, d, e): **, $P \leq 0.01$; ***, $P \leq 0.001$; ****, $P \leq 0.0001$. One-way AVOVA adjusted by Tukey's multiple comparison test was used in (c): *, $P \leq 0.05$; **, $P \leq 0.01$; ***, $P \leq 0.001$.



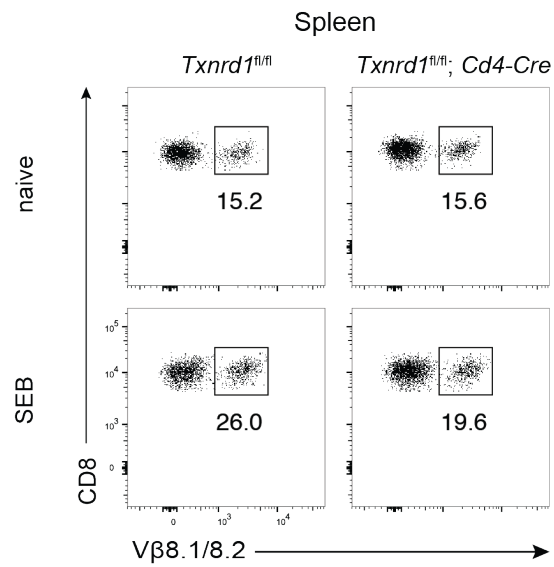
Supplementary Figure 3. T cells require *Txnrd1* for efficient expansion during LCMV infection. *Txnrd1^{fl/fl}* and *Txnrd1^{fl/fl};Cd4-Cre* mice were infected with 200 focus-forming units (FFU) LCMV WE i.v., and T cells in blood were analyzed after 3, 4 and 7 days of infection. **(a-b)** On day 7 of infection, activation of CD4⁺ and CD8⁺ T cells in blood was assessed by down-regulation of CD62L **(a)**, and virus-specific T cells were stained with gp₃₃₋₄₁ and gp₆₁₋₈₀ tetramers **(b)**. **(c)** Proliferation of splenic CD4⁺ T cells was assessed by EdU incorporation. Representative FACS plots (pre-gated on CD4⁺) and percentages of EdU⁺ cells are shown on the left and right side, respectively. **(d, e)** Cell death was assessed by staining with Annexin-V and 7-AAD, and percentages of alive (Annexin-V⁻ 7-AAD⁻) CD8⁺ **(d)** and CD4⁺ **(e)** T cells are shown (n=2-4). Means + standard deviations are shown. Data are representative of two independent experiments. Student's *t* test (two-tailed, unpaired) was used to compare *Txnrd1^{fl/fl}* and *Txnrd1^{fl/fl};Cd4-Cre* groups **(a-e)**: *, *P* ≤ 0.05; **, *P* ≤ 0.01; ***, *P* ≤ 0.001; ****, *P* ≤ 0.0001.



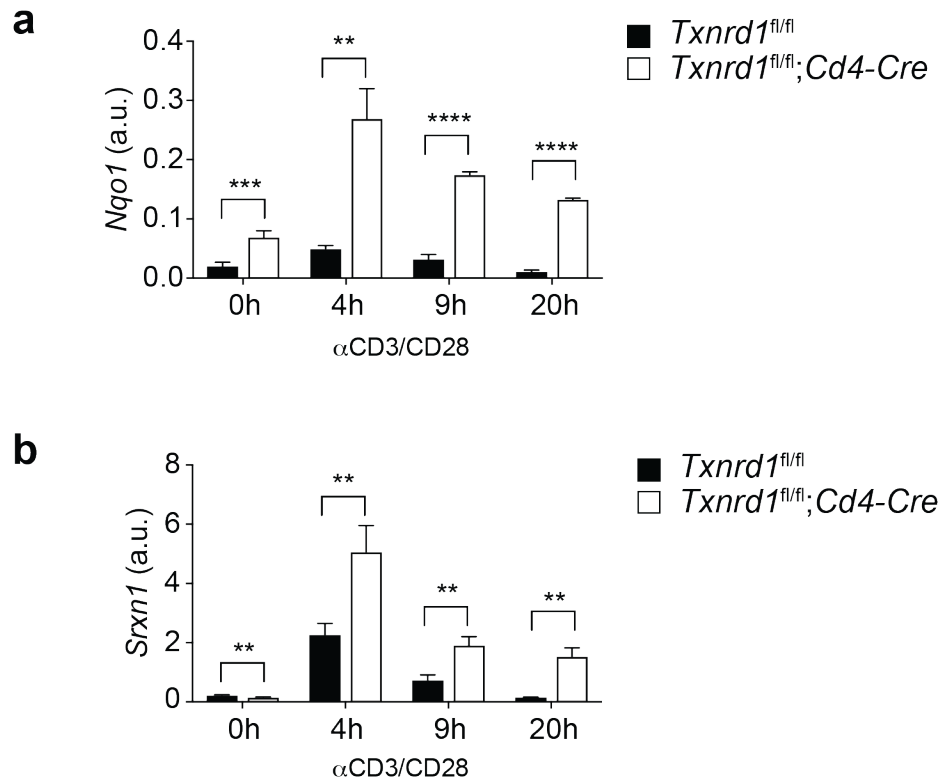
Supplementary Figure 4. *Txnrd1*-deficient T cells undergo longer cell cycling. Magnetically-sorted T cells from spleen and peripheral LNs of *Txnrd1^{fl/fl}* and *Txnrd1^{fl/fl};Cd4-Cre* mice were stimulated in α CD3/CD28-coated plates followed by flow cytometry analysis. (a) c-Myc protein expression level after 20 hours of T cells stimulation. (b) CFSE dilution of CD4⁺ T cells at the indicated times of stimulation. (c) CFSE-dilution profiles were used to calculate mean division time (t_{division} ; reciprocal of the slope) and time to first division ($t_{1^{\circ}\text{division}}$; intersection with mean division number $y = 1$) with the *precursor cohort method*. (d) CD4⁺ T cells leaving G₀ phase and entering cell cycle were detected by staining for Ki-67 at the indicated times of stimulation. Numbers in the plots indicate average percentage of Ki-67⁺ cells from triplicate samples. (e) CD4⁺ T cell death during α CD3/CD28 stimulation was assessed by staining cells with Annexin-V and 7-AAD. Representative FACS plots of cells stimulated for 1 day as well as quantification of alive (Annexin-V⁻ 7-AAD⁻) cells at the indicated times of stimulation (n=4). (f) Analysis of CD4⁺ T cell survival upon incubation with the indicated cell death inhibitors and antioxidants during 24 hours of α CD3/CD28 stimulation. Results for treatment with the ferroptosis inhibitors ciclopirox olamine (CPX; 8, 63, 500 nM), Deferoxamine (DFO; 1, 10, 50 μ M) and Ferrostatin-1 (Fer-1; 0.5, 2, 8 μ M); the necroptosis inhibitor Necrostatin-1 (Nec-1; 1, 4, 20 μ M) and the apoptosis inhibitor z-VAD-fmk (zVAD; 2, 12, 60 μ M) are shown in the left panel. Survival of T cells after addition of the antioxidants ascorbic acid (1, 6, 30 μ M) and α -Tocopherol (α Toc; 3, 16, 80 μ M) is shown in the right panel (n=2). (g) Representative FACS plots of ROS levels in unstimulated (left) and α CD3/CD28-stimulated T cells (right), stained with CM-H₂DCFDA. (h) T cells from WT (CD45.1⁺) and from *Txnrd1^{fl/fl};Cd4-Cre* mice (CD45.2⁺; or *Txnrd1^{fl/fl}* as control) were mixed at the indicated ratios (1:0, 0:1, 3:1, 1:1, 1:3) and stimulated for 3 days. Percentages of CD45.1⁺ (gray) and CD45.2⁺ (black) for CD4⁺ (top) and CD8⁺ (bottom) are shown (n=3). (i) Expression of indicated activation markers in CD4⁺ T cells measured by flow cytometry during the first 8h of stimulation (n=3). Bar graphs show mean + standard deviation. Data are representative of two (a, e-i), five (b), and three (c, d) independent experiments. Student's *t* test (two-tailed, unpaired) was used in (e): **, $P \leq 0.01$; ***, $P \leq 0.001$.



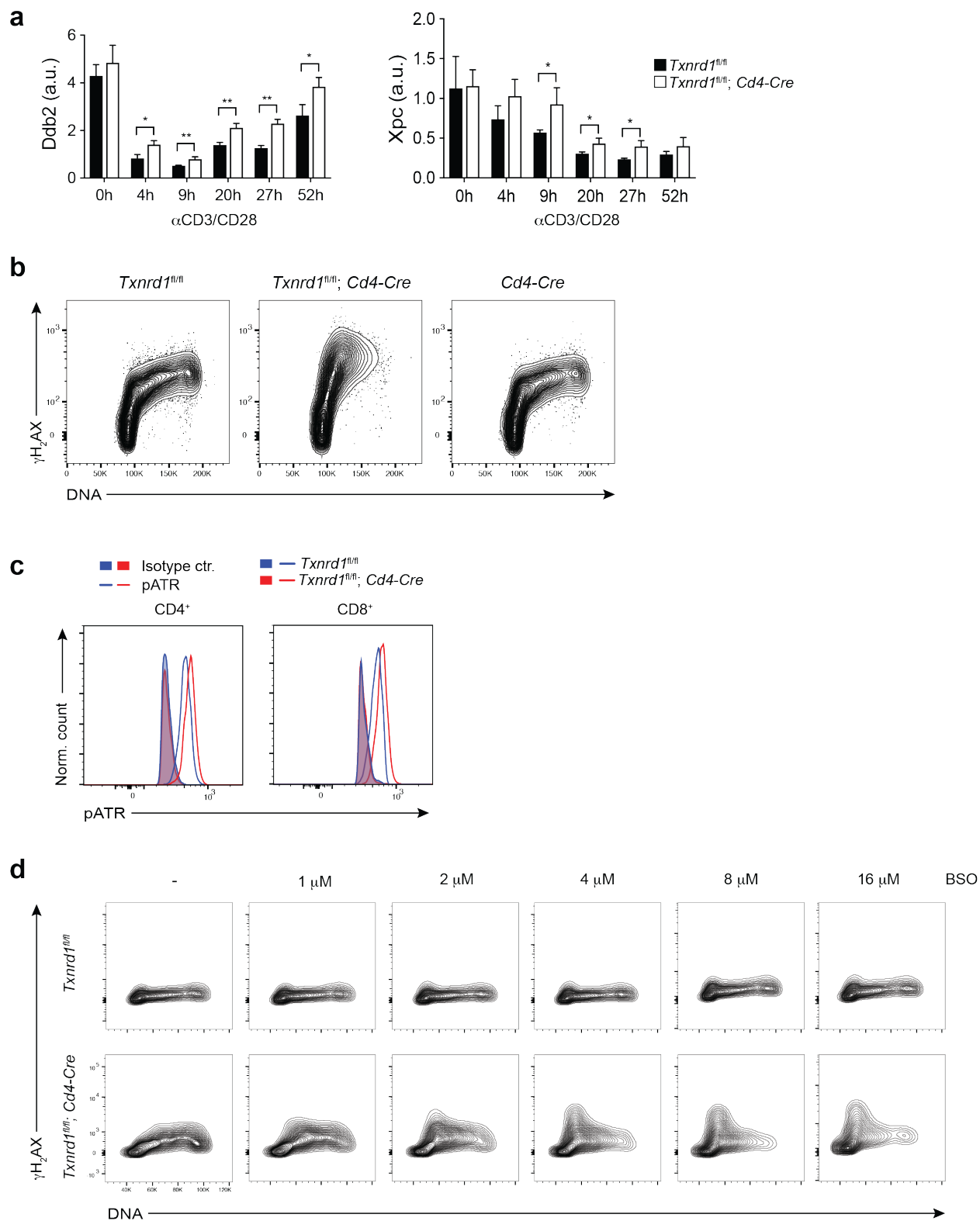
Supplementary Figure 5. *Txnrd1* deficiency leads to aspartate and glutamine/glutamate accumulation. Magnetically-sorted T cells from spleen and peripheral LNs of *Txnrd1^{fl/fl}* (WT) and *Txnrd1^{fl/fl};Cd4-Cre* mice (KO) were stimulated in α CD3/CD28-coated plates in vitro. **(a)** p-mTOR protein expression levels measured by flow cytometry after 48 hours of T cells stimulation. **(b-e)** Metabolites were analyzed by non-targeted metabolomics (four replicates were examined, each analyzed twice; as described for Fig. 5). **(b)** Volcano plots showing comparison of identified and annotated metabolites from stimulated (and unstimulated as control) WT and KO T cells. Closed circles indicate metabolites that changed significantly ($|\text{Log}_2(\text{fold-change})| > 0.5$; $p < 0.01$). **(c-e)** Box plots displaying aspartate, glutamine and glutamate **(c)**, glycolysis metabolites **(d)** and TCA cycle metabolite levels in WT and KO T cells **(e)**. Numbers in brackets represent the mass-to-charge ratio of the detected ions. Data are representative of two independent experiments. P-values of volcano plots were adjusted using Benjamini-Hochberg procedure **(b)**. The boxes represent the 25th to 75th percentiles, the horizontal lines within the boxes indicate the medians, and the whiskers are drawn to indicate the 1.5 x Inter Quartile Range (3rd quartile – 1st quartile; **c-e**). Student's *t* test (two-tailed, unpaired) corrected by the Benjamini-Hochberg multiple testing was used to compare WT and KO groups **(c-e)**.



Supplementary Figure 6. Representative FACS plots for Fig. 6b. *Txnrd1^{fl/fl}* and *Txnrd1^{fl/fl};Cd4-Cre* mice were treated i.p. with 100μg of SEB or PBS (naïve). Representative FACS plots showing Vβ8.1/8.2 expression of the CD8⁺ T cells, which were FACS-sorted for RNA-seq analysis (shown in Fig. 6).

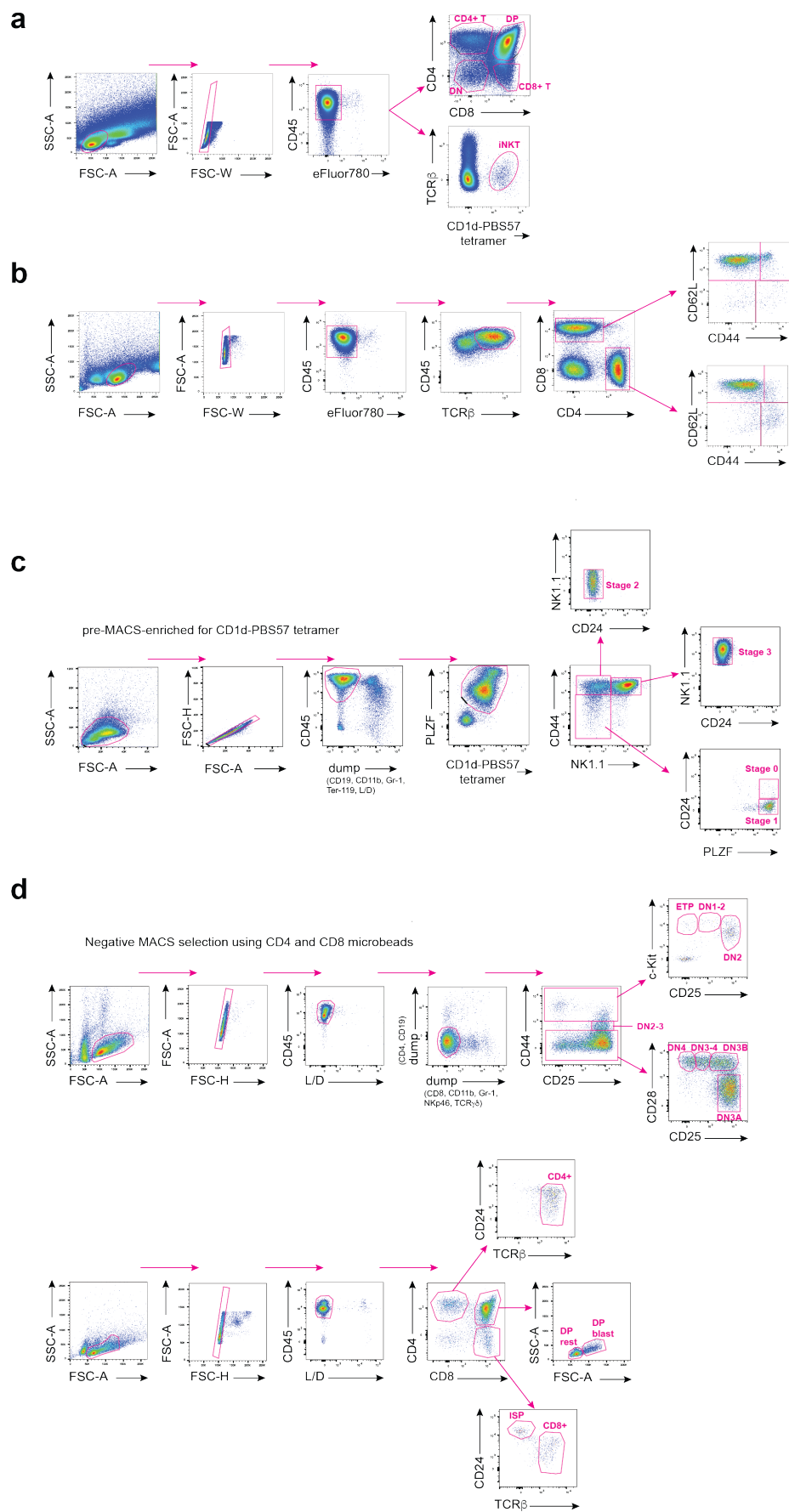


Supplementary Figure 7. Increased expression of Nrf2 target genes in *Txnrd1*-deficient T cells. (a-b) Magnetically-sorted T cells from spleen and peripheral LNs of naïve *Txnrd1*^{fl/fl} and *Txnrd1*^{fl/fl};Cd4-Cre mice were stimulated in α CD3/CD28-coated plates. *Nqo1* (a) and *Srxn1* (b) expression was assessed using RT-PCR at indicated times (n=3). Bar graphs show mean + standard deviation. Data are representative of two independent experiments. Student's *t* test (two-tailed, unpaired) was used to compare *Txnrd1*^{fl/fl} and *Txnrd1*^{fl/fl};Cd4-Cre groups: **, $P \leq 0.01$; ***, $P \leq 0.001$; ****, $P \leq 0.0001$.

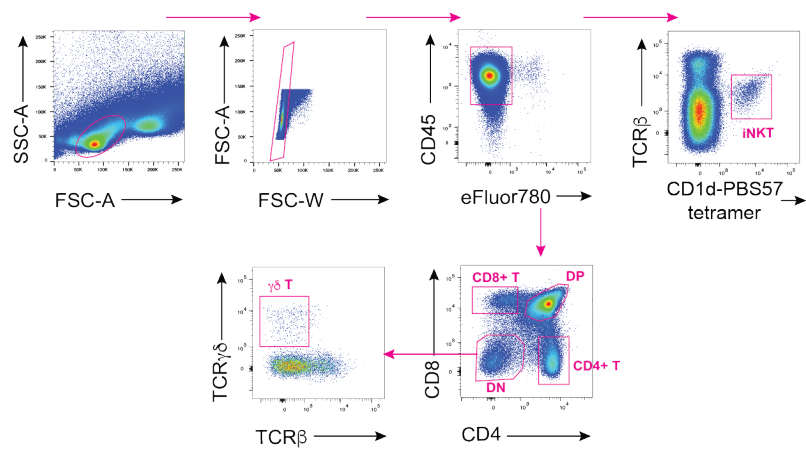
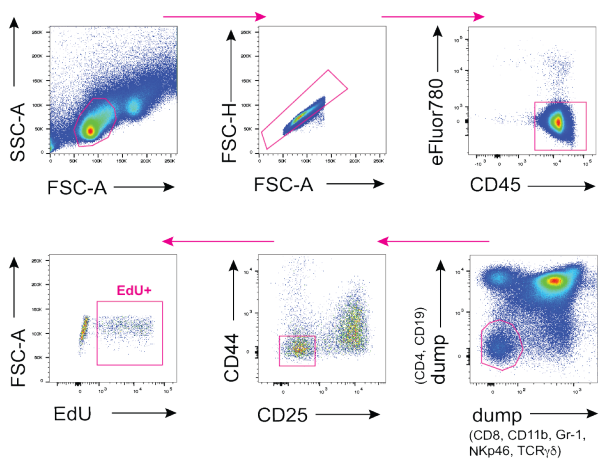
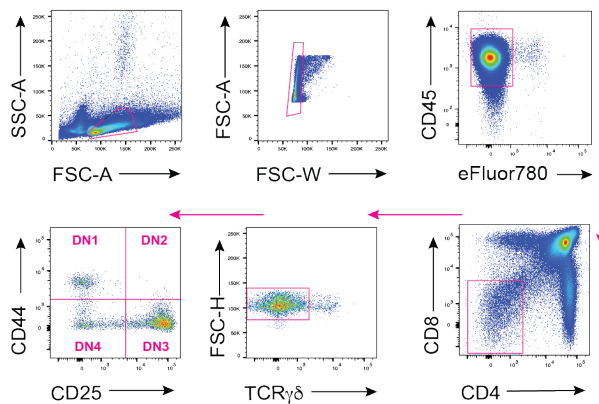


Supplementary Figure 8. *Txnrd1* deficiency leads to replication stress.

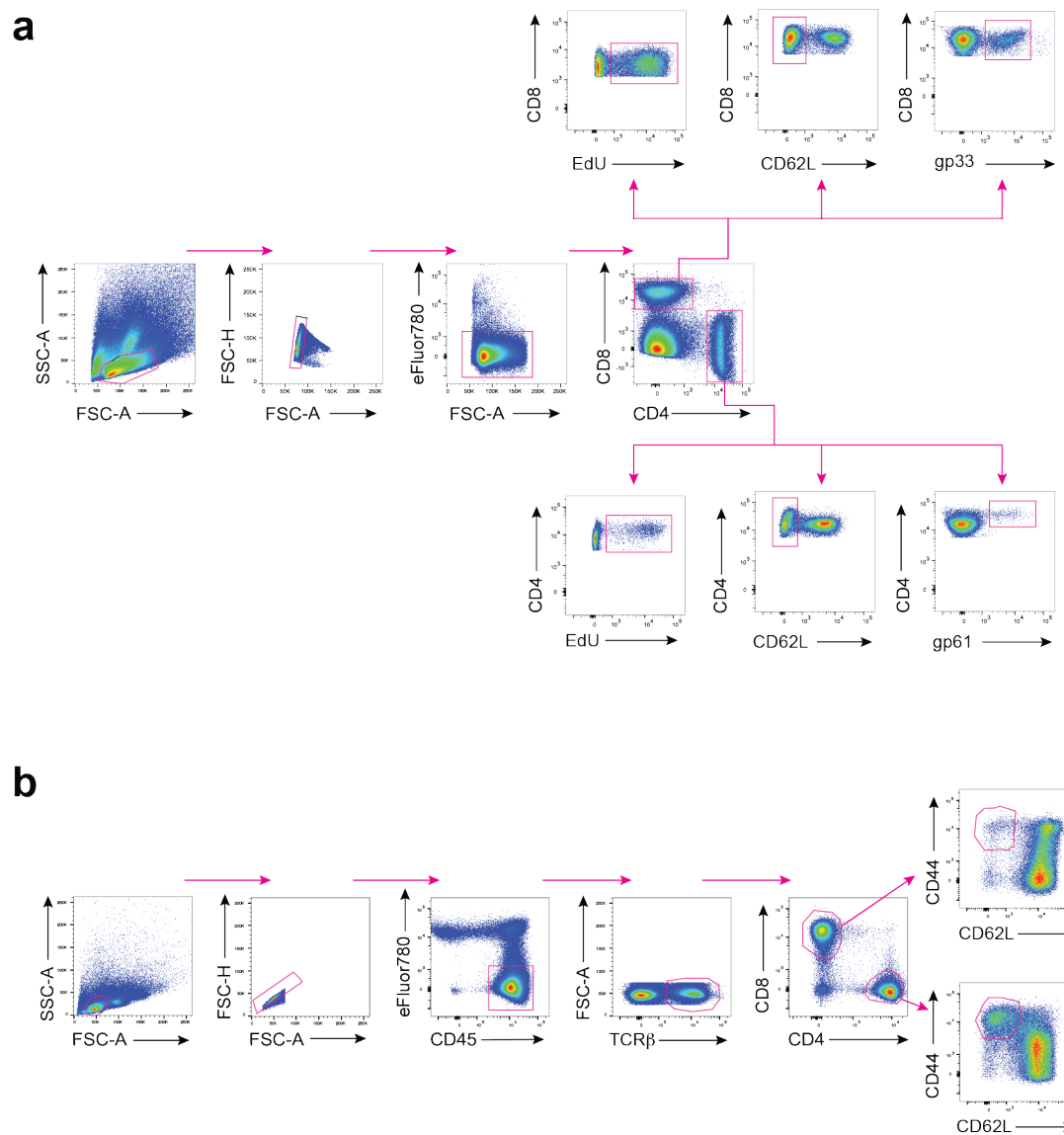
Magnetically-sorted T cells from spleen and peripheral LNs of *Txnrd1^{fl/fl}* and *Txnrd1^{fl/fl};Cd4-Cre* mice were stimulated in α CD3/CD28-coated plates in vitro. (a) *Ddb2* (left) and *Xpc* (right) expression levels in T cells determined by RT-PCR (n=3). (b) Representative FACS plots depicting γ H₂AX levels and DNA content in T cells from *Txnrd1^{fl/fl}* (left), *Txnrd1^{fl/fl};Cd4-Cre* (middle) and *Cd4-Cre* (right) mice after 30h of stimulation. (c) Representative FACS plots depicting pATR (S428) levels in T cells after 30h of stimulation (pre-gated on cells in the S-phase of the cell cycle). (d) Representative FACS plots depicting γ H₂AX levels and DNA content in T cells stimulated for 30h in the presence of the indicated concentrations of L-Buthionine-sulfoximine (BSO). Bar graphs show mean + standard deviation (a). Data are representative of two independent experiments. Student's *t* test (two-tailed, unpaired) was used to compare *Txnrd1^{fl/fl}* and *Txnrd1^{fl/fl};Cd4-Cre* groups (a): *, $P \leq 0.05$; **, $P \leq 0.01$.



Supplementary Figure 9. Gating strategies for Fig. 1 and Supplementary Fig. 1. (a-d) Representative FACS plots showing gating strategies for Fig. 1a, d, f and Supplementary Fig. 1a, b, g **(a)**; for Fig. 1b-e and Supplementary Fig. 1a-f **(b)**; for Fig. 1g **(c)**; and for Fig. 1h and Supplementary Fig. 1h **(d)**. For analysis of the different iNKT developmental stages, single thymi were MACS-enriched with APC-labeled CD1d-PBS57-tetramer and anti-APC microbeads **(c)**. Before FACS-sorting, DN thymocytes were enriched by negative selection using microbeads conjugated to anti-mouse CD4 and anti-mouse CD8 **(d; top)**.

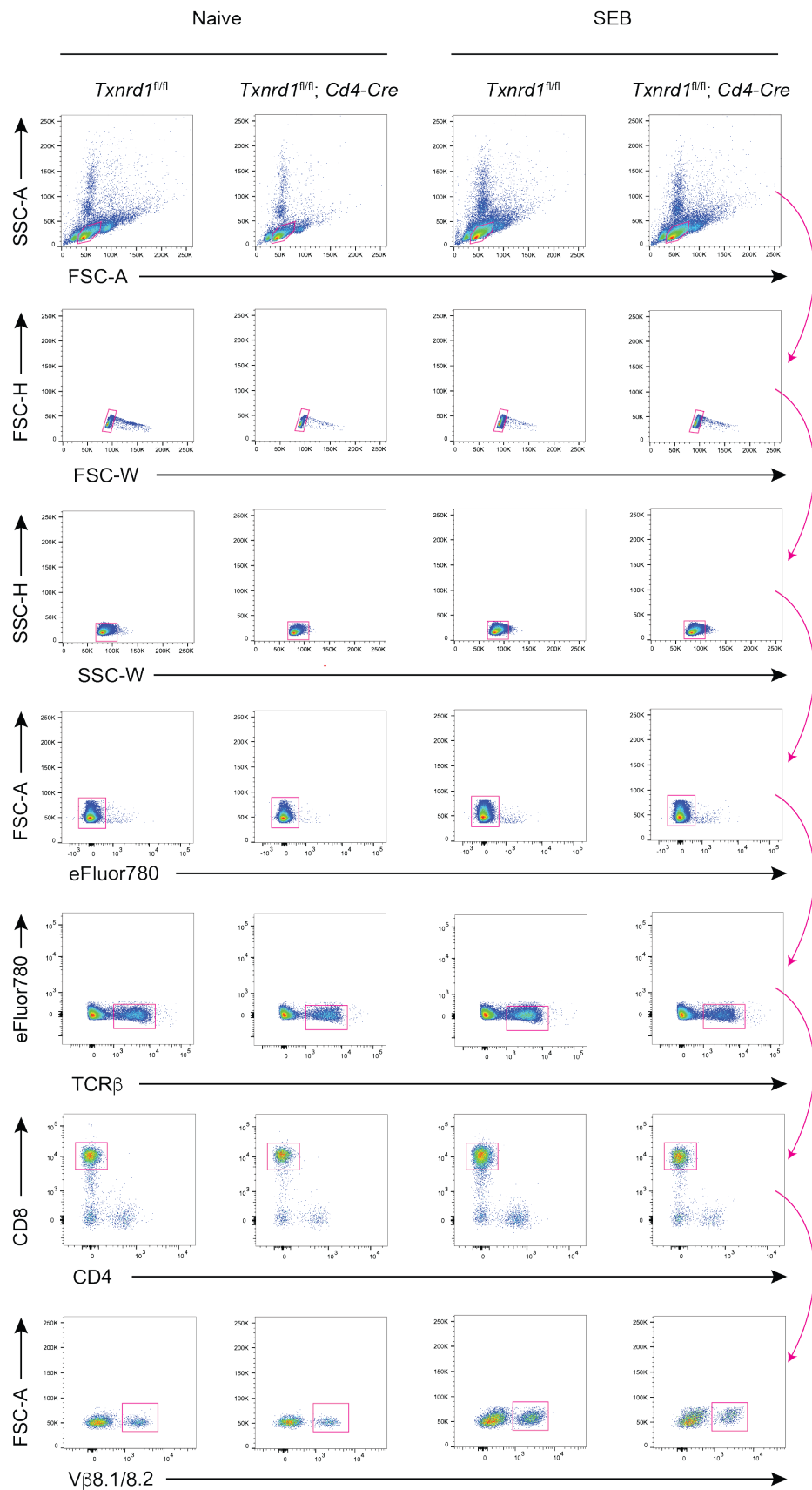
a**b****c**

Supplementary Figure 10. Gating strategies for Fig. 2 and Supplementary Fig. 2.
(a-c) Representative FACS plots showing gating strategies for Fig. 2c, d and Supplementary Fig. 2c **(a)**; for Fig. 2e **(b)**; and for Fig. 2f and Supplementary Fig. 2d **(c)**. CD4⁺ and CD8⁺ T cells depicted in Supplementary Fig. 2e were gated as described in Supplementary Fig. 9b.

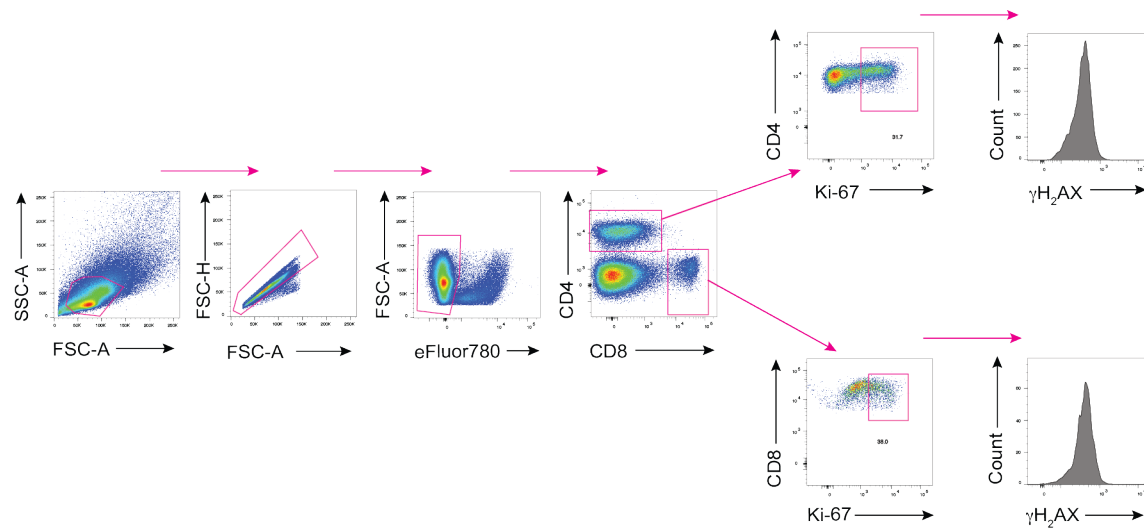


Supplementary Figure 11. Gating strategies for Fig. 3 and Supplementary Fig. 3.
(a-b) Representative FACS plots showing gating strategies for Fig. 3a-c and Supplementary Fig. 3a-c **(a)**; and for Fig. 3f, g **(b)**.

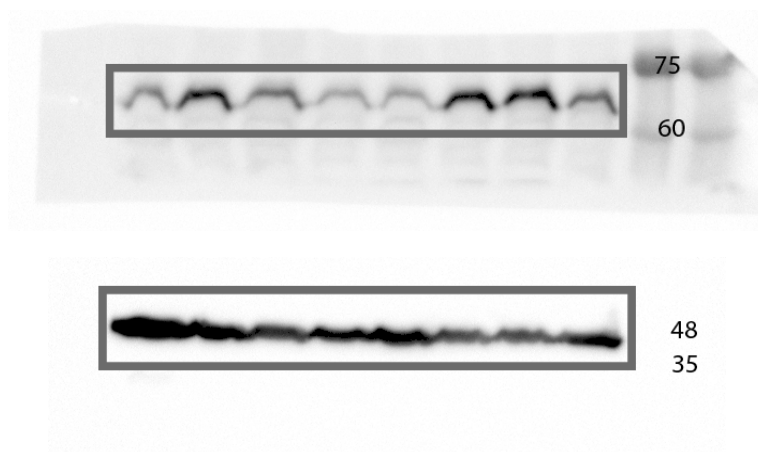
Negative MACS selection using CD4 and B220 microbeads



Supplementary Figure 12. Gating strategy for FACS-sorted SEB-stimulated CD8⁺ T cells used for RNA-seq in Fig. 6. Before FACS-sorting, splenic CD8⁺ T cells were enriched by negative selection using microbeads conjugated to anti-mouse CD4 and anti-mouse B220.



Supplementary Figure 13. Gating strategies for Fig. 7d. The first four FACS plots of the shown gating strategy were also used to gate CD4⁺ and CD8⁺ T cells for all the in vitro experiments.



Supplementary Figure 14. Uncropped Figure 5b. A molecular weight standard (kDa) is marked on the right.

Supplementary Tables

Supplementary Table 1. Single best predictor analysis of the RNA-seq data shown in Fig. 6. Linear regression model was performed to find the single best predictors in SEB-treated groups. Genes with *standard deviation* > 2 are depicted (genes were sorted according to descending standard deviation).

Gene	Std dev	R-squared
<i>Cdkn1a</i>	2.750	0.918
<i>Trav8d-2</i>	2.670	0.996
<i>Trav8n-2</i>	2.635	0.967
<i>Trav14d-3-dv8</i>	2.584	0.935
<i>Srxn1</i>	2.551	0.909
<i>Rapsn</i>	2.417	0.993
<i>Cxcl10</i>	2.362	0.926
<i>Trav10</i>	2.333	0.979
<i>Phf11d</i>	2.330	0.930
<i>Iqsec2</i>	2.303	0.997
<i>Ifitm1</i>	2.286	0.958
<i>S1pr5</i>	2.281	0.999
<i>Pdzd4</i>	2.250	0.910
<i>Trav7-4</i>	2.153	0.908
<i>Syne4</i>	2.139	0.945
<i>Palld</i>	2.125	1.000
<i>Trav7n-4</i>	2.086	0.970

Supplementary Table 2. Antibodies and staining reagents for flow cytometry.

Specificity	Conjugation	Clone	Supplier	Dilution
7-AAD	-	-	eBioscience	1:50
Annexin-V (for cell death)	APC	-	BD Bioscience	1:50
B220	PerCP	RA3-6B2	Biolegend	1:400
c-Myc	-	D84C12	Cell Signalling Technology	1:100
CD117	Biotin	2B8	Biolegend	1:200
CD19	APC-Cy7	6D5	Biolegend	1:800
CD19	PE	eBio1D3	eBioscience	1:500
CD23	PE	B3B4	eBioscience	1:300
CD25	PE	PC61	eBioscience	1:400
CD28	PE	E18	eBioscience	1:300
CD3e	PE	145-2C11	eBioscience	1:300
CD4	APC	GK1.5	BD Bioscience	1:1000
CD4	APC-Cy7	GK1.5	Biolegend	1:1000
CD4	FITC	GK1.5	eBioscience	1:800
CD4	PE	GK1.5	BD Bioscience	1:500
CD4	PE-Cy7	GK1.5	Biolegend	1:1000
CD4	PerCP-Cy5.5	RM4-5	Biolegend	1:500
CD11b	PE	M1/70	BD Bioscience	1:1000
CD44	Biotin	IM7	Biolegend	1:2000
CD44	PE	IM7	BD Bioscience	1:1000
CD44	PerCP-Cy5.5	IM7	eBioscience	1:500
CD45.1	APC	A20	Biolegend	1:100
CD45.1	Biotin	A20	BD Bioscience	1:200
CD45.2	APC	104	eBioscience	1:100
CD45.2	FITC	104	eBioscience	1:300
CD45.2	PE	104	eBioscience	1:200
CD45.2	PE-Cy7	104	Biolegend	1:200
CD62L	APC	MEL-14	Biolegend	1:200
CD62L	FITC	MEL-14	eBioscience	1:500
CD62L	PE	MEL-14	BD Bioscience	1:500
CD69	FITC	H1.2F3	Biolegend	1:300
CD71	FITC	R17217	eBioscience	1:200
CD8	APC	53-6.7	eBioscience	1:600
CD8	FITC	53-6.7	eBioscience	1:600
CD8	PE	53-6.7	Biolegend	1:2000
CD8	PE-Cy7	53-6.7	Biolegend	1:1000
CD8	PerCP	53-6.7	Biolegend	1:600
eFluor® 780	-	-	eBioscience	1:2000
Fc Block CD16/32	-	2.4G2	Home-made	1:1000
FxCycle Violet Stain	-	-	Thermo Scientific	1:400
Gr-1	PE	RB6-8C5	Biolegend	1:800
Ki-67	PE	16A8	Biolegend	1:1000
LIVE/DEAD® fixable-yellow-dead-cell-stain	-	-	Life Technology	1:500
NK1.1	PE	PK136	eBioscience	1:300
Phospho-ATR (Ser428)	-	-	Cell Signalling Technology	1:100
Phospho-H ₂ AX (Ser139)	AF488	N1-431	BD Bioscience	1:400
Phospho-mTOR (Ser2448)	PE	MRRBY	eBioscience	1:100
PLZF	PE	9E12	Biolegend	1:1000
Rabbit-IgG(H+L)	FITC	-	SouthernBiotech	1:500
Streptavidin	APC	-	eBioscience	1:1000
Streptavidin	APC-Cy7	-	Biolegend	1:1000
Streptavidin	BV711	-	BD Bioscience	1:1000
Streptavidin	PE-Cy7	-	Biolegend	1:1000
Streptavidin	PerCP	-	Biolegend	1:500
TCR β	APC	H57-597	Biolegend	1:500
TCR β	PE-Cy7	H57-597	BD Bioscience	1:1000
TCR $\gamma\delta$	Biotin	GL3	BD Bioscience	1:300
Ter-119	PE	TER-119	eBioscience	1:100
Vb8.1/8.2	FITC	KJ16-133	eBioscience	1:50

Supplementary Table 3. Sequences of primers used for RT-PCR.

Target gene	Primer sequences
<i>Cdkn1a</i>	Forward: 5'-AGACCAGCCTGACAGATTTC-3' Reverse: 5'-CTGACCCACAGCAGAAGAG-3'
<i>c-Myc</i>	Forward: 5'-TTGAAGGCTGGATTCCTTTGGGC-3' Reverse: 5'-TCGTTCGCAGATGAAATAGGGCTGT-3'
<i>Ddb2</i>	Forward: 5'-GGCAAGGAGCTTTGGAAC-3' Reverse: 5'-GTTTGATCTATGGAGGCTGTG-3'
<i>Grx1</i>	Forward: 5'-TGCAGAAAGACCCAAGAAATCCTCAGTCA-3' Reverse: 5'-TGGAGATTAGATCACTGCATCCGCCTATG-3'
<i>Nqo1</i>	Forward: 5'-GGTGATATTTCAGTTCCCATTG-3' Reverse: 5'-ACTCTCTCAAACCAGCCTTTC-3'
<i>Srxn1</i>	Forward: 5'-GGTGGACACGATCCTGGCGG-3' Reverse: 5'-GGTAGGCTGCATAGCGGTGGC-3'
<i>Txn1</i>	Forward: 5'-ATGACTGCCAGGATGTTGC-3' Reverse: 5'-CCTTGTTAGCACCGGAGAAC-3'
<i>Txnip</i>	Forward: 5'-CCTGACCTAATGGCACCAG-3' Reverse: 5'-AGGAATGAACATGCAGGAAAC-3'
<i>Txnrd1</i>	Forward: 5'-AAAGACGATGAACGTGTCTG-3' Reverse: 5'-CTTAGTCAGCCCACACTTGAG-3'
<i>Txnrd1</i> DNA	Forward: 5'-ACAGGAGTGATCCCCACAGACC-3' Reverse: 5'-CTGGAACCGCCCTGAATATCACC-3'
<i>Txnrd1</i> mRNA in KO	Forward: 5'-GCTGACTAAGCAGCAGCTGG-3' Reverse: 5'-AACCTCAGCAGCCAGACTGG-3'
<i>Xpc</i>	Forward: 5'-GCAAGAAGGCAAAGAAACAC-3' Reverse: 5'-TTCAGTAAGCTCTCCACCTC-3'
<i>Tbp</i> (housekeeping for mRNA)	Forward: 5'-TTGACCTAAAGACCATTGCACTTC-3' Reverse: 5'-TTCTCATGATGACTGCAGCAAA-3'
<i>Txnrd1</i> (housekeeping for DNA)	Forward: 5'-ACAGATCGAAGCAGGAACAC-3' Reverse: 5'-TTCAGAGAGGAAAGTCACCC-3'

Supplementary Table 4. MRM settings used for targeted metabolomics.

Metabolite	Q1	Q2
AMP	346	134
GMP	362	79
dATP	490	159
dGTP	506	79